Int. J. Anal. Appl. (2026), 24:277

International Journal of Analysis and Applications

A Flexible Sine-Transformed Extension of the Nakagami Distribution

Parawan Pijitrattana[1], **Ibrahim Abdullahi**[2,*]

[1]*Department of Mathematics and Statistics, Faculty of Science and Technology, Thammasat University, Thailand*

[2]*Department of Mathematics and Statistics, Yobe State University Damaturu, Nigeria*

Corresponding author: ibworld82@yahoo.com

Abstract. A central problem in distribution theory is the construction of flexible models that retain analytical tractability while improving shape adaptability in applications. We propose a sine-transformed extension of the Nakagami distribution by applying a trigonometric mapping to the baseline cumulative distribution function. The resulting sine-transformed Nakagami model preserves the original two-parameter structure, admits closed-form expressions for both the distribution and density functions, and yields tractable reliability measures. We establish key structural properties, including validity, smoothness, and well-defined support; in addition, a hazard modulation representation relative to the classical Nakagami model is derived; and obtain explicit upper-tail asymptotics showing that the proposed transformation preserves the light-tailed class while modifying survival decay in a controlled and interpretable manner. Series representations are developed to facilitate the computation of moments and other related functionals. Parameters are estimated by maximum likelihood using numerical optimization, and finite-sample performance is evaluated through Monte Carlo simulation studies. Applications to real data illustrate that the sine-transformed Nakagami distribution provides an improved goodness of fit compared with the classical Nakagami model for reliability-type data.

1. Introduction

The development of flexible probability distributions remains a fundamental and crucial topic in distribution theory and applied statistics, primarily because real-world data is inherently diverse and complex. Although classical parametric models are widely utilized due to their analytical tractability and computational simplicity, they frequently lack the necessary flexibility to accurately accommodate the complex skewness, unusual tail behaviors, or time-varying hazard-rate dynamics commonly observed in empirical data. This limitation has motivated the introduction of

Received: Jul. 4, 2026.

2020 *Mathematics Subject Classification.* 62E15, 62E10.

Key words and phrases. Sine-generated distributions; Trigonometric transformation; Hazard modulation; Tail asymptotics; Flexible lifetime models.

https://doi.org/10.28924/2291-8639-24-2026-277

ISSN: 2291-8639

generator-based extensions that enrich baseline distributions while preserving inferential feasibility. Early foundational work in this area includes exponentiated families [14], the Marshall–Olkin transformation [12], and the beta-generated class [8], which provided unprecedented control over data skewness and tail weights. Further developments in generalized lifetime modeling addressed computational constraints and expanded analytical capabilities. The Kumaraswamy-G [7] and McDonald-G [2] families improved mathematical tractability and successfully accommodated non-monotonic hazard rates. A major paradigm shift subsequently occurred with the T–X family [3, 11]. By allowing any continuous random variable T to act as a generator for a baseline variable X via a specific link function $W(F(x))$, this generalized framework opened the door to virtually infinite modeling possibilities.

Recently, trigonometric generators have emerged as an appealing alternative for introducing additional flexibility without excessive algebraic complexity. Bounded periodic transformations, particularly sine-based constructions, have been shown to modify hazard curvature and tail behavior in a controlled manner. General trigonometric frameworks and specific sine-generated families have been developed and successfully applied to reliability and lifetime modeling [1, 13, 18, 20].

The Nakagami distribution is a cornerstone model in wireless communications, signal processing, medical imaging, and reliability analysis. Owing to its connection with the gamma distribution, it supports efficient likelihood-based inference and stable computation [9, 10, 15]. While several generalizations of the Nakagami model have been introduced to enhance its flexibility in applied contexts [4, 5, 17], the classical Nakagami structure remains governed by a single shape parameter. This limitation may restrict its adaptability when empirical data exhibit subtle departures in hazard dynamics or tail decay.

Although sine-based generators have been studied within general distributional frameworks, their structural impact on the Nakagami distribution has not been systematically examined. In particular, the implications of a trigonometric transformation on hazard behavior, tail characteristics, and likelihood-based inference within the Nakagami setting remain underexplored. To address this gap, we introduce a sine-transformed Nakagami (SS-Nakagami) distribution that modifies the cumulative structure while preserving the original two-parameter framework. Unlike many generator-based extensions that increase model dimensionality, the proposed model enhances shape flexibility without introducing additional parameters, thereby maintaining parsimony and interpretability.

We derive closed-form expressions for the density and distribution functions and establish key structural properties, including survival and hazard functions, series representations, moments, entropy, and order statistics. Parameter estimation is conducted via maximum likelihood, and finite-sample performance is investigated through simulation studies. Applications to real-world reliability datasets illustrate the practical advantages of the proposed model.

2. The Proposed Distribution

The probability density function (PDF) of a Nakagami-distributed random variable Y is given by the following formula:

$$g(y;m,\Omega)=\frac{2m^m}{\Gamma(m)\Omega^m}y^{2m-1}exp\left(-\frac{m}{\Omega}y^2\right)\quad y>0.$$

Let $G(y;m,\Omega)$ denote the Nakagami cumulative distribution function (CDF),

$$G(y;m,\Omega)=\frac{\gamma\left(m,\frac{m}{\Omega}y^2\right)}{\Gamma(m)}\quad y>0, \tag{2.1}$$

where $m>\frac{1}{2}$ and $\Omega>0$ represent the shape and scale parameters, respectively. In this expression, $\Gamma(z)=\int_0^\infty t^{z-1}e^{-t}dt$ denotes the complete gamma function, and $\gamma(s,z)=\int_0^z t^{s-1}e^{-t}dt$ represents the lower incomplete gamma function.

Definition 2.1. *The cumulative distribution function of the SS-Nakagami distribution is defined by*

$$F(y;m,\Omega)=\sin\left(\frac{\pi}{2}G(y;m,\Omega)\right) \tag{2.2}$$

Substituting Equation (2.1) into (2.2) yield

$$F(y;m,\Omega)=\sin\left(\frac{\pi}{2}\frac{\gamma\left(m,\frac{m}{\Omega}y^2\right)}{\Gamma(m)}\right)\quad y>0, \tag{2.3}$$

where $m>\frac{1}{2}$ and $\Omega>0$. Since $0\leq\frac{\gamma\left(m,\frac{m}{\Omega}y^2\right)}{\Gamma(m)}\leq 1$, the argument of the sine function strictly falls within $\left[0,\frac{\pi}{2}\right]$. It follows that $F(0)=0$, $F(\infty)=1$, and $F(y;m,\Omega)$ is monotonically non-decreasing, confirming it is a valid CDF. Figure 1 illustrates the plots of the CDF of the SS-Nakagami distribution. The left panel demonstrates the effect of varying the shape parameter m, while the right panel shows how changes in the scale parameter Ω influence the distribution.

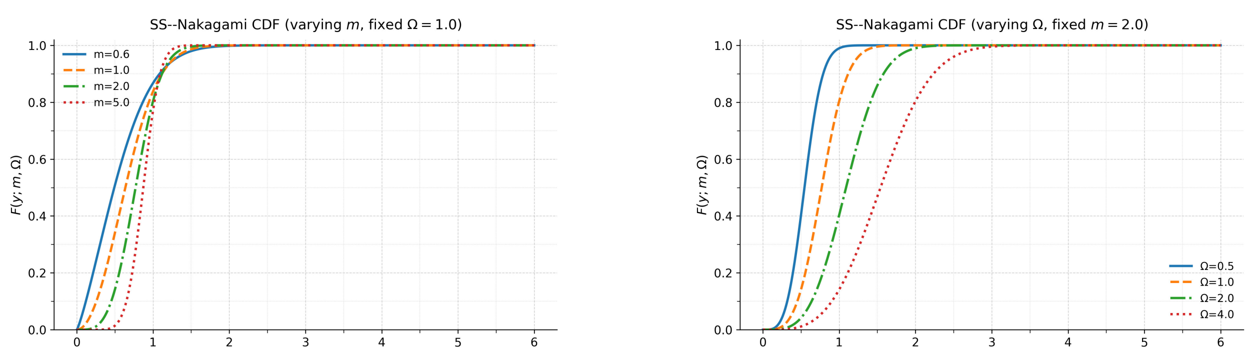

Figure 1. Cumulative distribution function of the SS-Nakagami distribution : (left) varying shape parameter m, and (right) varying scale parameter Ω.

The probability density function in (2.4) is obtained by differentiating the distribution function in (2.3) with respect to y.

$$
\begin{aligned}
f(y;m,\Omega) &= \frac{\pi m^m}{\Gamma(m)\Omega^m} y^{2m-1} \exp\!\left(-\frac{m}{\Omega}y^2\right) \cos\!\left[\frac{\pi}{2}\frac{\gamma\left(m, \frac{m}{\Omega}y^2\right)}{\Gamma(m)}\right] \\
&= \frac{\pi}{2} g(y;m,\Omega)\cos\left(\frac{\pi}{2}G(y;m,\Omega)\right) \qquad y > 0,
\end{aligned} \tag{2.4}
$$

for all $m > \frac{1}{2}$ and $\Omega > 0$.

Proof. Since $G(y;m,\Omega)$ is the CDF of Nakagami distribution, $0 \le G(y;m,\Omega) \le 1$, $G(0^+) = 0$ and $\lim_{y\to\infty} G(y;m,\Omega) = 1$, implying $F(0^+) = 0$ and $\lim_{y\to\infty} F(y;m,\Omega) = 1$.

By differentiating (2.2),

$$
F'(y;m,\Omega) = \frac{\pi}{2} G'(y;m,\Omega)\cos\!\left(\frac{\pi}{2}G(y;m,\Omega)\right), \tag{2.5}
$$

where

$$
G'(y;m,\Omega) = \frac{2m^m}{\Gamma(m)\Omega^m} y^{2m-1} \exp\!\left(-\frac{m}{\Omega}y^2\right).
$$

Hence (2.5) coincides with (2.4). Since $0 \le \frac{\pi}{2}G(y;m,\Omega) \le \frac{\pi}{2}$, $f(y;m,\Omega) \ge 0$ for all $y > 0$, and

$$
\int_0^\infty f(y;m,\Omega)\,dy = F(\infty) - F(0^+) = 1.
$$

Thus (2.4) is a valid probability density function. □

Figure 2 presents the PDF of the SS-Nakagami distribution. The left panel highlights the impact of varying the shape parameter m, whereas the right panel illustrates how changes in the scale parameter Ω affect the distribution.

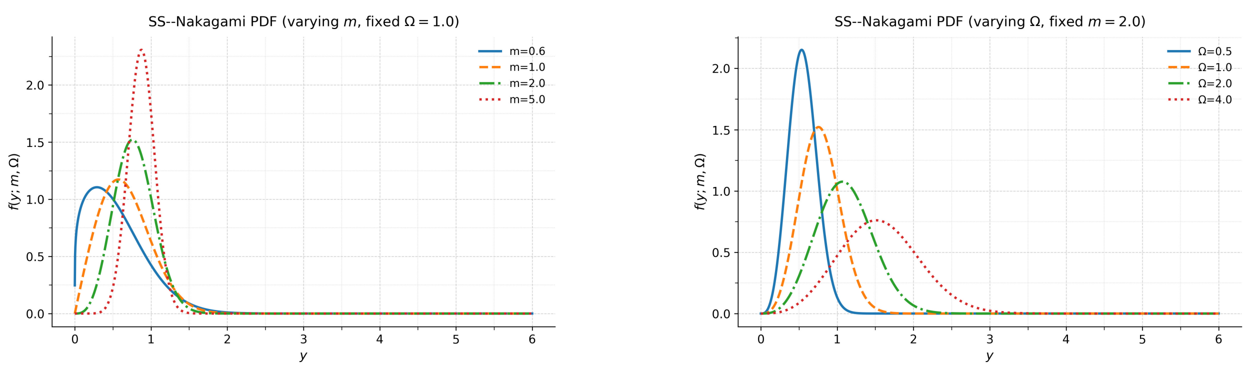

Figure 2. Probability density function of the SS-Nakagami distribution: (left) varying shape parameter m, and (right) varying scale parameter Ω.

3. Survival and Hazard Rate Functions

This section develops the principal reliability characteristics of the SS-Nakagami distribution, including the survival function, hazard rate function, a structural hazard modulation representation, and tail asymptotics relative to the classical Nakagami model.

3.1. **Survival Function.** Let $Y \sim$ SS-Nakagami(m, Ω) with cumulative distribution function given in (2.1). The survival function is defined by

$$S(y) = \Pr(Y > y) = 1 - F(y),$$

where $F(y)$ is the CDF. Hence,

$$S(y; m, \Omega) = 1 - \sin\left(\frac{\pi}{2} G(y; m, \Omega)\right) \qquad y > 0, \tag{3.1}$$

where $m > \frac{1}{2}$ and $\Omega > 0$.

The sine transformation modifies the decay structure of the baseline Nakagami survival function while preserving smoothness and monotonicity. Figure 3 illustrates the influence of m and Ω on survival behavior.

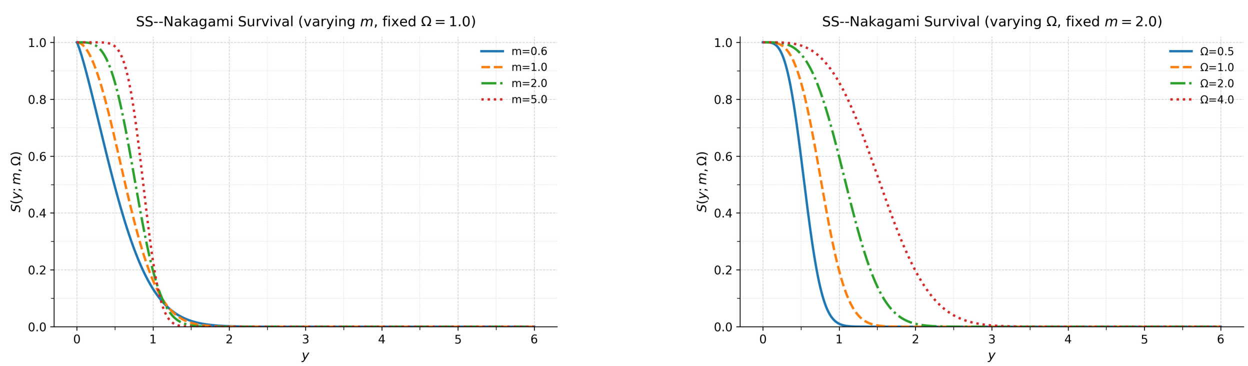

Figure 3. Survival functions of the SS-Nakagami distribution: (left) varying shape parameter m, and (right) varying scale parameter Ω.

3.2. **Hazard Rate Function.** The hazard rate (failure rate) function is defined as

$$h(y) = \frac{f(y)}{S(y)},$$

where $f(y)$ and $S(y)$ denote the probability density function and the survival function, respectively. Using the density given in (2.4) and the survival function in (3.1), the hazard rate can be written as

$$h(y; m, \Omega) = \frac{\frac{\pi}{2} g(y; m, \Omega) \cos\left(\frac{\pi}{2} G(y; m, \Omega)\right)}{1 - \sin\left(\frac{\pi}{2} G(y; m, \Omega)\right)} \qquad y > 0,$$

where $m > \frac{1}{2}$ and $\Omega > 0$. The hazard function inherits the structural stability of the baseline distribution but gains additional non-linear flexibility from the trigonometric transformation.

This enables the model to accommodate increasing, bathtub, or unimodal hazard shapes, as demonstrated by the varying parameter values of m and Ω in Figure 4.

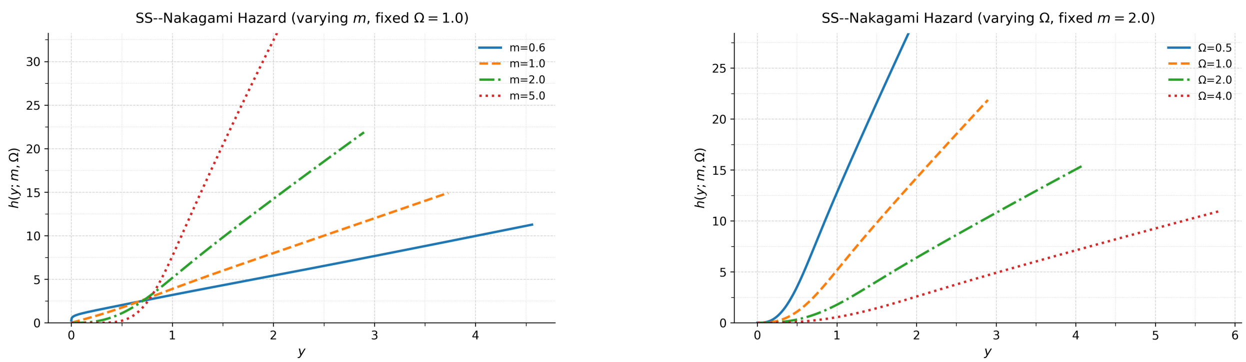

Figure 4. Hazard functions of the SS-Nakagami distribution: (left) varying shape parameter m, and (right) varying scale parameter Ω.

3.3. **Structural Hazard Modulation.** The following result shows that the SS-Nakagami hazard is a multiplicative modification of the classical Nakagami hazard function.

Theorem 3.1. *Let $Y \sim$ Nakagami(m, Ω) with hazard function*

$$\lambda(y; m, \Omega) = \frac{g(y; m, \Omega)}{\overline{G}(y; m, \Omega)},$$

where $\overline{G}(y; m, \Omega) = 1 - G(y; m, \Omega)$. If $Y \sim$ SS-Nakagami(m, Ω), then the modulated hazard rate function is given by

$$h_{SSN}(y; m, \Omega) = \lambda(y; m, \Omega)\, R(y; m, \Omega),$$

where

$$R(y; m, \Omega) = \frac{\pi}{2} \frac{\overline{G}(y; m, \Omega) \cos\left(\frac{\pi}{2} G(y; m, \Omega)\right)}{1 - \sin\left(\frac{\pi}{2} G(y; m, \Omega)\right)}.$$

This representation shows that the sine transformation acts as a bounded multiplicative modulation of the baseline hazard. In particular, as $y \to \infty$, $G(y; m, \Omega) \to 1$ and $\overline{G}(y; m, \Omega) \to 0$, yielding

$$h_{SSN}(y; m, \Omega) \sim 2\, \lambda(y; m, \Omega) \qquad y \to \infty,$$

demonstrating controlled hazard amplification in the upper tail.

3.4. **Tail Behavior and Asymptotic Structure.** The sine transformation preserves the exponential-type decay class of the Nakagami distribution while modifying the survival magnitude.

Theorem 3.2 (Tail behavior preservation)**.** *Let $X \sim$ Nakagami(m, Ω) with survival $\overline{G}(y; m, \Omega)$ and let $Y \sim$ SS-Nakagami(m, Ω) with survival $\overline{F}_{SSN}(y; m, \Omega)$. Then*

$$\overline{F}_{SSN}(y; m, \Omega) = 1 - \cos\Big(\frac{\pi}{2}\overline{G}(y; m, \Omega)\Big).$$

Moreover, as $y \to \infty$,

$$\overline{F}_{SSN}(y; m, \Omega) \sim \frac{\pi^2}{8}\,\overline{G}(y; m, \Omega)^2.$$

Thus

$$\log \overline{F}_{SSN}(y; m, \Omega) = 2 \log \overline{G}(y; m, \Omega) + O(1),$$

where $O(1)$ represents a constant term that is independent of y.

Proof. Since $G(y; m, \Omega) = 1 - \overline{G}(y; m, \Omega)$,

$$F_{SSN}(y; m, \Omega) = \sin\Big(\frac{\pi}{2}(1 - \overline{G}(y; m, \Omega))\Big) = \cos\Big(\frac{\pi}{2}\overline{G}(y; m, \Omega)\Big).$$

Thus

$$\overline{F}_{SSN}(y; m, \Omega) = 1 - \cos\Big(\frac{\pi}{2}\overline{G}(y; m, \Omega)\Big).$$

As $\overline{G}(y; m, \Omega) \to 0$ as $y \to \infty$, using $1 - \cos t \sim t^2/2$ as $t \to 0$ gives the stated asymptotic result. □

Theorem 3.2 shows that the SS-Nakagami distribution remains within the same light-tailed class as the classical Nakagami model while introducing a quadratic refinement in survival decay. Thus, the transformation enhances curvature without altering the fundamental exponential tail structure.

4. Linear Representation and Properties

Let $G(y) = G(y; m, \Omega)$ denote the Nakagami cumulative distribution function and $g(y) = G'(y)$ be the corresponding probability density function.

4.1. **Linear (Series) Representation.** Using the power series expansion

$$\cos x = \sum_{k=0}^{\infty} \frac{(-1)^k x^{2k}}{(2k)!},$$

with $x = \frac{\pi}{2}G(y)$, the cosine term in the SS-Nakagami probability density function can be expanded as

$$\cos\Big(\frac{\pi}{2}G(y)\Big) = \sum_{k=0}^{\infty} \frac{(-1)^k}{(2k)!}\left(\frac{\pi}{2}\right)^{2k} G(y)^{2k}.$$

Since

$$f(y;m,\Omega) = \frac{\pi}{2} g(y) \cos\Big(\frac{\pi}{2} G(y)\Big),$$

it follows that the SS-Nakagami density admits the linear representation

$$f(y;m,\Omega) = \sum_{k=0}^{\infty} a_k\, g(y)\, G(y)^{2k} \quad y > 0, \tag{4.1}$$

where

$$a_k = \frac{\pi}{2} \frac{(-1)^k}{(2k)!} \Big(\frac{\pi}{2}\Big)^{2k}, \qquad k = 0, 1, 2, \ldots.$$

This representation expresses the proposed model as an infinite linear combination of weighted Nakagami densities.

4.2. **Moments.** Let $r > -2m$. Using the Equation (4.1) and interchanging summation and integration, the rth raw moment of Y is given by

$$E(Y^r) = \sum_{k=0}^{\infty} a_k \int_0^{\infty} y^r g(y)\, G(y)^{2k}\, dy.$$

Equivalently, letting $Y_0 \sim \text{Nakagami}(m, \Omega)$ and using the probability integral transform $U = G(Y_0) \sim \text{Uniform}(0,1)$, one obtains

$$E(Y^r) = \sum_{k=0}^{\infty} a_k \int_0^{1} \Big(Q_{\text{Nak}}(u)\Big)^r u^{2k}\, du, \tag{4.2}$$

where $Q_{\text{Nak}}(\cdot)$ denotes the Nakagami quantile function.

4.3. **Mean and Variance.** Using the Equation (4.2), the mean of the SS-Nakagami distribution is

$$\mu = E(Y) = \sum_{k=0}^{\infty} a_k \int_0^{1} Q_{\text{Nak}}(u)\, u^{2k}\, du. \tag{4.3}$$

Similarly, the second raw moment is

$$E(Y^2) = \sum_{k=0}^{\infty} a_k \int_0^{1} \Big(Q_{\text{Nak}}(u)\Big)^2 u^{2k}\, du. \tag{4.4}$$

Substituting the Equation (4.3) and (4.4) into the variance identity $\text{Var}(Y) = E(Y^2) - \mu^2$ yields

$$\text{Var}(Y) = \sum_{k=0}^{\infty} a_k \int_0^{1} \Big(Q_{\text{Nak}}(u)\Big)^2 u^{2k}\, du - \left(\sum_{k=0}^{\infty} a_k \int_0^{1} Q_{\text{Nak}}(u)\, u^{2k}\, du\right)^2.$$

4.4. **Moment Generating Function.** Using Equation (4.2), the moment generating function (MGF) of the SS-Nakagami distribution is

$$M_Y(t) = \mathbb{E}\Big(e^{tY}\Big) = \int_0^\infty e^{ty}\, f(y;m,\Omega)\, dy.$$

Substituting the linear representation

$$f(y;m,\Omega) = \sum_{k=0}^{\infty} a_k\, g(y)\, G(y)^{2k},$$

and interchanging summation and integration (justified by dominated convergence), we obtain

$$M_Y(t) = \sum_{k=0}^{\infty} a_k \int_0^\infty e^{ty}\, g(y)\, G(y)^{2k}\, dy. \tag{4.5}$$

Equivalently, by the probability integral transform $U = G(Y_0) \sim U(0,1)$ for $Y_0 \sim$ Nakagami(m,Ω), one may write

$$M_Y(t) = \sum_{k=0}^{\infty} a_k \int_0^1 \exp\Big(t\, Q_{\text{Nak}}(u)\Big)\, u^{2k}\, du, \tag{4.6}$$

where $Q_{\text{Nak}}(\cdot)$ denotes the Nakagami quantile function.

4.5. **Mode.** The mode of the SS-Nakagami distribution is obtained by maximizing the density $f(y;m,\Omega)$ in Equation (2.4). Since $f(y;m,\Omega) > 0$ for $y > 0$, the mode y^* is obtained as follows

$$\frac{d}{dy}\log f(y;m,\Omega) = 0.$$

Using

$$f(y;m,\Omega) = \frac{\pi}{2}\, g(y;m,\Omega)\, \cos\Big(\frac{\pi}{2} G(y;m,\Omega)\Big),$$

we write

$$\log f(y;m,\Omega) = \log\Big(\frac{\pi}{2}\Big) + \log g(y;m,\Omega) + \log\cos\Big(\frac{\pi}{2} G(y;m,\Omega)\Big). \tag{4.7}$$

Differentiating (4.7) with respect to y yields

$$\frac{d}{dy}\log f(y;m,\Omega) = \frac{2m-1}{y} - \frac{2m}{\Omega}y - \frac{\pi}{2}\, g(y;m,\Omega)\, \tan\Big(\frac{\pi}{2} G(y;m,\Omega)\Big),$$

where

$$g(y;m,\Omega) = \frac{2m^m}{\Gamma(m)\Omega^m}\, y^{2m-1} \exp\Big(-\frac{m}{\Omega}y^2\Big).$$

Consequently, the mode y^* satisfies the nonlinear equation

$$\frac{2m-1}{y} - \frac{2m}{\Omega}y - \frac{\pi}{2}\, g(y;m,\Omega)\, \tan\Big(\frac{\pi}{2} G(y;m,\Omega)\Big) = 0 \qquad y > 0. \tag{4.8}$$

Equation (4.8) can be solved numerically using standard root-finding methods (e.g., Newton-Raphson or bisection). A convenient initial value is the mode of the classical Nakagami distribution (for $m > \frac{1}{2}$),

$$y_0 = \sqrt{\frac{\Omega(2m-1)}{2m}}.$$

4.6. **Quantile Function.** Let $0 < u < 1$. The quantile function $Q(u) = F^{-1}(u)$ corresponding to the CDF in Equation (2.3) is obtained by solving $F(y) = u$ for y.

From Equation (2.3), we have

$$u = \sin\left(\frac{\pi}{2}\frac{\gamma\left(m, \frac{m}{\Omega}y^2\right)}{\Gamma(m)}\right).$$

Taking the inverse sine function gives

$$\arcsin(u) = \frac{\pi}{2}\frac{\gamma\left(m, \frac{m}{\Omega}y^2\right)}{\Gamma(m)}.$$

Hence,

$$\frac{\gamma\left(m, \frac{m}{\Omega}y^2\right)}{\Gamma(m)} = \frac{2}{\pi}\arcsin(u).$$

Let $P(m, x) = \gamma(m, x)/\Gamma(m)$ denote the regularized incomplete gamma function. Then,

$$P\left(m, \frac{m}{\Omega}y^2\right) = \frac{2}{\pi}\arcsin(u).$$

Applying the inverse of $P(m, x)$ with respect to its second argument yields

$$\frac{m}{\Omega}y^2 = P^{-1}\left(m, \frac{2}{\pi}\arcsin(u)\right).$$

Therefore, the quantile function is

$$Q(u) = \sqrt{\frac{\Omega}{m}P^{-1}\left(m, \frac{2}{\pi}\arcsin(u)\right)}, \qquad 0 < u < 1. \tag{4.9}$$

4.7. **Entropy.** The Shannon entropy of the SS-Nakagami distribution is defined as

$$H(Y) = -E[\log f(Y)] = -\int_0^\infty f(y; m, \Omega)\log f(y; m, \Omega)\,dy.$$

Using the logarithmic form of the density given in (4.7), together with (4.1) and the probability integral transform, the entropy can be expressed as

$$H(Y) = -\log\left(\frac{\pi}{2}\right) - \sum_{k=0}^{\infty} a_k \int_0^1 \log g\left(Q_{\text{Nak}}(u)\right) u^{2k}\,du$$
$$- \sum_{k=0}^{\infty} a_k \int_0^1 \log\left[\cos\left(\frac{\pi}{2}u\right)\right] u^{2k}\,du,$$

where $Q_{\text{Nak}}(\cdot)$ denotes the Nakagami quantile function.

4.8. **Order Statistics.** Let $Y_{1:n} \leq \cdots \leq Y_{n:n}$ denote the order statistics from a random sample of size n drawn from the SS-Nakagami distribution. The density of the rth order statistic is

$$f_{r:n}(y) = \frac{n!}{(r-1)!(n-r)!}[F(y)]^{r-1}[1-F(y)]^{n-r}f(y), \quad y > 0.$$

Here, $F(y) = F(y; m, \Omega)$ denotes the CDF of SS-Nakagami distribution, and $f(y) = f(y; m, \Omega)$ denotes the corresponding PDF. Substituting the linear representations of $F(y)$ and $f(y)$ yields

$$f_{r:n}(y) = \frac{n!}{(r-1)!(n-r)!}\left(\sum_{\ell=0}^{n-r}(-1)^{\ell}\binom{n-r}{\ell}F(y)^{r-1+\ell}\right)\left(\sum_{k=0}^{\infty}a_k g(y)G(y)^{2k}\right),$$

which provides a convenient form for numerical evaluation and further theoretical analysis.

5. Parameter Estimation

In this section, the parameters of the SS-Nakagami distribution are estimated using the maximum likelihood method.

Let $Y_1, \ldots, Y_n$ be a random sample from the SS-Nakagami distribution with probability density function given in Equation (2.4). The likelihood function is defined as follows:

$$L(m, \Omega) = \prod_{i=1}^{n} f(y_i; m, \Omega),$$

where $f(y_i; m, \Omega)$ is defined in (2.4).

The corresponding log-likelihood function is given by

$$\ell(m, \Omega) = n\log\pi + nm\log m - n\log\Gamma(m) - nm\log\Omega + (2m-1)\sum_{i=1}^{n}\log y_i$$
$$-\frac{m}{\Omega}\sum_{i=1}^{n}y_i^2 + \sum_{i=1}^{n}\log\left[\cos\left(\frac{\pi}{2}G(y_i; m, \Omega)\right)\right],$$

where $G(y_i; m, \Omega)$ is given in Equation (2.1).

The maximum likelihood estimators $(\widehat{m}, \widehat{\Omega})$ are obtained by solving

$$\frac{\partial\ell(m, \Omega)}{\partial m} = 0, \qquad \frac{\partial\ell(m, \Omega)}{\partial\Omega} = 0.$$

Since these equations do not admit closed-form solutions, numerical optimization methods, such as the BFGS quasi-Newton algorithm, are employed.

Under standard regularity conditions, the MLE satisfies

$$\sqrt{n}\begin{pmatrix}\widehat{m} - m \\ \widehat{\Omega} - \Omega\end{pmatrix} \xrightarrow{d} \mathcal{N}\left(\begin{pmatrix}0 \\ 0\end{pmatrix}, \mathcal{I}^{-1}(m, \Omega)\right),$$

where $\mathcal{I}(m, \Omega)$ denotes the Fisher information matrix.

6. Performance of the Maximum Likelihood Estimators

This section examines the finite-sample performance of the maximum likelihood estimators (MLEs) for the SS-Nakagami distribution through Monte Carlo simulation. Random samples were generated using the inverse transform method based on the quantile function in Equation (4.9). Specifically, if $U \sim \text{Uniform}(0,1)$, then

$$Y = Q(U)$$

follows the SS-Nakagami(m, Ω) distribution.

The log-likelihood function was maximized numerically using the BFGS quasi-Newton algorithm implemented in the `maxLik` package in `R`. Convergence diagnostics were monitored in all replications to ensure numerical stability.

The simulation study was conducted for parameter values $m \in \{0.8, 1.2, 2, 3, 5\}$ with fixed scale parameter $\Omega = 1.5$. Sample sizes were taken as

$$n \in \{10, 30, 50, 100, 500\}.$$

For each (m, n) configuration, $R = 1{,}000$ Monte Carlo replications were performed.

6.1. **Monte Carlo Simulation Design.** For each fixed (n, m, Ω), the simulation procedure was as follows:

(1) Generate $U_i \overset{iid}{\sim} \text{Uniform}(0,1)$, $i = 1, \ldots, n$, and set

$$Y_i = Q(U_i),$$

where $Q(\cdot)$ denotes the SS-Nakagami quantile function.

(2) Compute the MLE $(\widehat{m}_r, \widehat{\Omega}_r)$ by numerically maximizing

$$\ell(m, \Omega) = \sum_{i=1}^{n} \log f(Y_i; m, \Omega).$$

(3) Obtain the observed information matrix $\widehat{\mathcal{I}}(\widehat{m}_r, \widehat{\Omega}_r)$ via the negative Hessian at the MLE and compute standard errors as

$$\widehat{\text{SE}}(\widehat{m}_r) = \sqrt{\left[\widehat{\mathcal{I}}^{-1}\right]_{11}}, \qquad \widehat{\text{SE}}(\widehat{\Omega}_r) = \sqrt{\left[\widehat{\mathcal{I}}^{-1}\right]_{22}}.$$

(4) Repeat Steps 1-3 for $r = 1, \ldots, R$.

Let $\widehat{\theta}_r$ denote the estimate of $\theta \in \{m, \Omega\}$ from the rth replication, and define

$$\overline{\widehat{\theta}} = \frac{1}{R} \sum_{r=1}^{R} \widehat{\theta}_r.$$

The empirical performance measures are

$$\text{Bias}(\widehat{\theta}) = \overline{\widehat{\theta}} - \theta,$$

$$\mathrm{Var}(\widehat{\theta}) = \frac{1}{R-1}\sum_{r=1}^{R}\left(\widehat{\theta}_r - \overline{\widehat{\theta}}\right)^2,$$

$$\mathrm{MSE}(\widehat{\theta}) = \frac{1}{R}\sum_{r=1}^{R}\left(\widehat{\theta}_r - \theta\right)^2.$$

By construction,

$$\mathrm{MSE}(\widehat{\theta}) = \mathrm{Var}(\widehat{\theta}) + \mathrm{Bias}(\widehat{\theta})^2.$$

6.2. **Coverage Probability of Wald Confidence Intervals.** In addition to bias and MSE, the empirical coverage probabilities of the nominal $(1-\alpha)100\%$ Wald confidence intervals were evaluated for $\theta \in \{m, \Omega\}$, with $\alpha = 0.05$.

For each replication,

$$\mathrm{CI}_r(\theta) = \left[\widehat{\theta}_r - z_{1-\alpha/2}\widehat{\mathrm{SE}}(\widehat{\theta}_r),\ \widehat{\theta}_r + z_{1-\alpha/2}\widehat{\mathrm{SE}}(\widehat{\theta}_r)\right],$$

where $z_{1-\alpha/2}$ denotes the $1-\alpha/2$ quantile of the standard normal distribution and $\widehat{\mathrm{SE}}(\widehat{\theta}_r)$ is the estimated standard error.

The empirical coverage probability is

$$\mathrm{CP}(\theta) = \frac{1}{R}\sum_{r=1}^{R}\mathbf{1}\{\theta \in \mathrm{CI}_r(\theta)\},$$

where $\mathbf{1}\{\cdot\}$ denotes the indicator function, which takes the value 1 if the condition $\theta \in \mathrm{CI}_r(\theta)$ is true and 0 otherwise.

The average interval length is

$$\mathrm{AvgLen} = \frac{1}{R}\sum_{r=1}^{R}\mathrm{Length}(\mathrm{CI}_r(\theta)),$$

where $\mathrm{Length}(\mathrm{CI}_r(\theta))$ represents the width of the interval calculated in the r-th simulation.

Tables 1-5 summarize the Monte Carlo performance of the MLEs for increasing sample sizes $n \in \{10, 30, 50, 100, 500\}$, across varying true values of m with fixed $\Omega = 1.5$. For small samples ($n = 10$), a noticeable upward bias is observed for the shape parameter m, particularly for larger true values. This bias diminishes steadily as n increases. By $n = 100$ and $n = 500$, the bias becomes negligible across all parameter settings, indicating strong finite-sample consistency.

Table 1. Monte Carlo performance of the MLEs for $n = 10$ under varying true values of m ($\Omega = 1.5$).

	Parameter m						Parameter Ω					
m	Mean	Bias	Var	MSE	CP	AvgLen	Mean	Bias	Var	MSE	CP	AvgLen
0.8	1.0277	0.2277	0.3590	0.4096	0.9733	1.4702	1.4498	-0.0502	0.2944	0.2959	0.8600	1.9974
1.2	1.5942	0.3942	0.7382	0.8911	0.9700	2.4167	1.4383	-0.0617	0.1577	0.1609	0.8633	1.5175
2.0	2.7324	0.7324	1.8897	2.4198	0.9698	4.3306	1.4403	-0.0597	0.0833	0.0865	0.8624	1.1084
3.0	4.0526	1.0526	4.9178	6.0092	0.9428	6.6955	1.4971	-0.0029	0.0700	0.0697	0.8889	0.9436
5.0	6.4391	1.4391	8.6605	10.7001	0.9239	11.0694	1.4917	-0.0083	0.0404	0.0403	0.8986	0.7148

Table 2. Monte Carlo performance of the MLEs for $n = 30$ under varying true values of m ($\Omega = 1.5$).

	Parameter m						Parameter Ω					
m	Mean	Bias	Var	MSE	CP	AvgLen	Mean	Bias	Var	MSE	CP	AvgLen
0.8	0.8588	0.0588	0.0391	0.0424	0.9400	0.6851	1.4972	-0.0028	0.0993	0.0989	0.9067	1.2228
1.2	1.2924	0.0924	0.0842	0.0928	0.9667	1.1075	1.4868	-0.0132	0.0558	0.0559	0.9267	0.8923
2.0	2.2422	0.2422	0.2992	0.3579	0.9500	2.0196	1.4817	-0.0183	0.0324	0.0328	0.9267	0.6682
3.0	3.2402	0.2402	0.5378	0.5955	0.9592	3.0895	1.4954	-0.0046	0.0214	0.0214	0.9327	0.5425
5.0	5.5223	0.5223	1.7531	2.0251	0.9487	5.4305	1.4944	-0.0056	0.0120	0.0120	0.9051	0.4067

Table 3. Monte Carlo performance of the MLEs for $n = 50$ under varying true values of m ($\Omega = 1.5$).

	Parameter m						Parameter Ω					
m	Mean	Bias	Var	MSE	CP	AvgLen	Mean	Bias	Var	MSE	CP	AvgLen
0.8	0.8365	0.0365	0.0223	0.0236	0.9500	0.5137	1.5120	0.0120	0.0576	0.0575	0.9367	0.9599
1.2	1.2521	0.0521	0.0471	0.0496	0.9633	0.8109	1.4822	-0.0178	0.0352	0.0354	0.9300	0.7356
2.0	2.1089	0.1089	0.1867	0.1979	0.9467	1.4498	1.4955	-0.0045	0.0193	0.0193	0.9300	0.5515
3.0	3.1213	0.1213	0.3828	0.3962	0.9500	2.2241	1.5016	0.0016	0.0130	0.0129	0.9333	0.4441
5.0	5.3445	0.3445	1.1886	1.3033	0.9498	3.9906	1.4879	-0.0121	0.0077	0.0076	0.9130	0.3282

Table 4. Monte Carlo performance of the MLEs for $n = 100$ under varying true values of m ($\Omega = 1.5$).

	Parameter m						Parameter Ω					
m	Mean	Bias	Var	MSE	CP	AvgLen	Mean	Bias	Var	MSE	CP	AvgLen
0.8	0.8223	0.0223	0.0086	0.0091	0.9600	0.3559	1.4971	-0.0029	0.0312	0.0311	0.9400	0.6706
1.2	1.2248	0.0248	0.0180	0.0185	0.9500	0.5551	1.4958	-0.0042	0.0183	0.0183	0.9367	0.5116
2.0	2.0552	0.0552	0.0716	0.0747	0.9500	0.9878	1.5015	0.0015	0.0104	0.0104	0.9300	0.3836
3.0	3.0683	0.0683	0.1508	0.1554	0.9467	1.5247	1.4985	-0.0015	0.0070	0.0070	0.9200	0.3096
5.0	5.1773	0.1773	0.4580	0.4894	0.9398	2.7596	1.4972	-0.0028	0.0041	0.0041	0.9100	0.2285

Table 5. Monte Carlo performance of the MLEs for $n = 500$ under varying true values of m ($\Omega = 1.5$).

	Parameter m						Parameter Ω					
m	Mean	Bias	Var	MSE	CP	AvgLen	Mean	Bias	Var	MSE	CP	AvgLen
0.8	0.8036	0.0036	0.0017	0.0017	0.9500	0.1549	1.4884	-0.0116	0.0061	0.0062	0.9300	0.3000
1.2	1.2006	0.0006	0.0034	0.0034	0.9500	0.2361	1.4998	-0.0002	0.0036	0.0036	0.9200	0.2295
2.0	2.0110	0.0110	0.0133	0.0134	0.9500	0.4195	1.5001	0.0001	0.0020	0.0020	0.9100	0.1719
3.0	3.0086	0.0086	0.0264	0.0265	0.9500	0.6422	1.4999	-0.0001	0.0014	0.0014	0.9100	0.1386
5.0	5.0347	0.0347	0.0812	0.0824	0.9500	1.1562	1.4995	-0.0005	0.0008	0.0008	0.9000	0.1021

The empirical variances decrease monotonically with sample size, and the MSE exhibits an approximate $O(n^{-1})$ rate of decay, consistent with the asymptotic likelihood theory developed in Section 5.

As sample sizes increase, coverage probabilities converge toward the nominal 95% level. For the scale parameter Ω, the MLE demonstrates superior performance with minimal bias and variance across all configurations; notably, coverage remains stable even at small n. The narrowing of average confidence interval lengths further validates the estimators' increasing precision as n grows.

Overall, the results demonstrate stable numerical performance, asymptotic consistency, and reliable interval estimation properties for the SS-Nakagami maximum likelihood estimators.

6.3. **Application.** The first data were originally obtained by researchers at the UK National Physical Laboratory and have been widely used in reliability and lifetime modeling studies. The dataset has been previously analyzed by [19] and [6] primarily within the framework of Weibull and generalized Weibull-type distributions. The data represent the tensile strength of glass fibres with a diameter 1.5 cm and consist of 63 positive observations: 0.55, 0.93, 1.25, 1.36, 1.49, 1.52, 1.58, 1.61, 1.64, 1.68, 1.73, 1.81, 2.00, 0.74, 1.04, 1.27, 1.39, 1.49, 1.53, 1.59, 1.61, 1.66, 1.68, 1.76, 1.82, 2.01, 0.77, 1.11, 1.28, 1.42, 1.50, 1.54, 1.60, 1.62, 1.66, 1.69, 1.76, 1.84, 2.24, 0.81, 1.13, 1.29, 1.48, 1.50, 1.55, 1.61, 1.62, 1.66, 1.70, 1.77, 1.84, 0.84, 1.24, 1.30, 1.48, 1.51, 1.55, 1.61, 1.63, 1.67, 1.70, 1.78, 1.89. The data are strictly positive and moderately right-skewed with a clear unimodal structure.

Table 6. MLEs and goodness-of-fit comparison for the glass fibre tensile strength data.

Measure	**Nakagami**	**SS-Nakagami**
$\hat{m}$	5.0427	4.3396
$\widehat{SE}(\hat{m})$	0.8921	0.8015
$\hat{\Omega}$	2.3739	3.0487
$\widehat{SE}(\hat{\Omega})$	0.3124	0.4287
$\ell(\hat{m}, \hat{\Omega})$	-20.8435	**-18.4405**
AIC	45.6870	**40.8811**
BIC	49.9733	**45.1673**
KS Statistic (D)	0.2030	**0.1861**
KS p-value	0.0094	0.0221
Anderson-Darling (AD)	2.5413	**2.0342**
Cramér-von Mises (CVM)	0.4695	**0.3690**

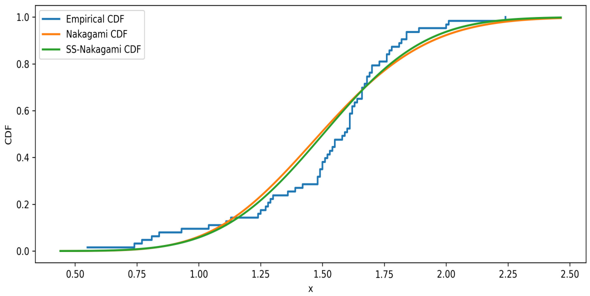

(a) Glass: Empirical and fitted CDFs

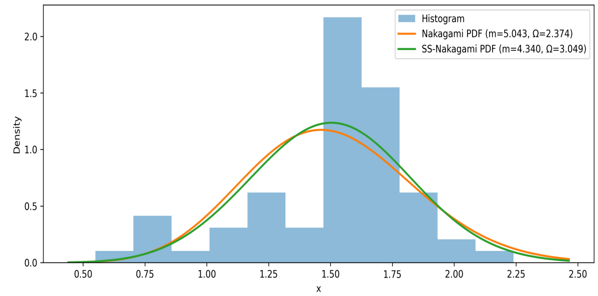

(b) Glass: Histogram with fitted PDFs

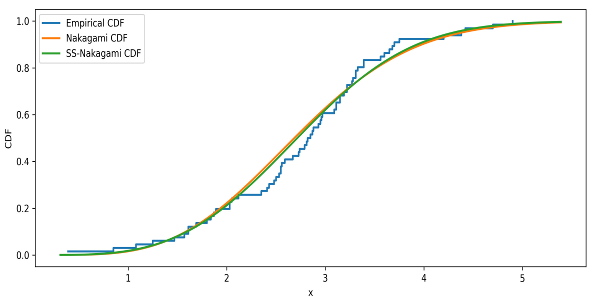

(c) Carbon: Empirical and fitted CDFs

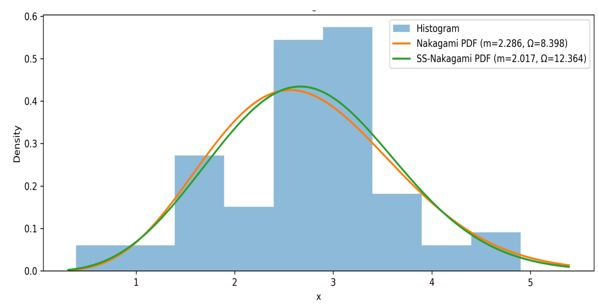

(d) Carbon: Histogram with fitted PDFs

FIGURE 5. Empirical and fitted distributions for the glass fibres and carbon fibres datasets.

TABLE 7. MLEs and goodness-of-fit comparison for the breaking stress of carbon fibres data.

Measure	**Nakagami**	**SS-Nakagami**
$\hat{m}$	2.2864	2.0172
$\widehat{SE}(\hat{m})$	0.2856	0.2638
$\hat{\Omega}$	8.3977	12.3643
$\widehat{SE}(\hat{\Omega})$	1.1243	1.5321
$\ell(\hat{m}, \hat{\Omega})$	-87.8554	**-86.7525**
AIC	179.7107	**177.5049**
BIC	184.0900	**181.8842**
KS Statistic (D)	0.1105	**0.0960**
KS p-value	0.3692	0.5454
Anderson-Darling (AD)	0.8261	**0.6175**
Cramér-von Mises (CVM)	0.1592	**0.1159**

The second empirical dataset concerns the breaking stress of carbon fibres with a length 50 mm, measured in gigapascals (GPa). The dataset has been previously analyzed by [16] and [17] in reliability and lifetime modeling contexts. The data consist of 66 positive observations: 0.39, 0.85, 1.08, 1.25, 1.47, 1.57, 1.61, 1.61, 1.69, 1.80, 1.84, 1.87, 1.89, 2.03, 2.03, 2.05, 2.12, 2.35, 2.41, 2.43, 2.48, 2.50, 2.53, 2.55, 2.55, 2.56, 2.59, 2.67, 2.73, 2.74, 2.79, 2.81, 2.82, 2.85, 2.87, 2.88, 2.93, 2.95, 2.96, 2.97, 3.09, 3.11, 3.11, 3.15, 3.15, 3.19, 3.22, 3.22, 3.27, 3.28, 3.31, 3.31, 3.33, 3.39, 3.39, 3.56, 3.60, 3.65, 3.68, 3.70, 3.75, 4.20, 4.38, 4.42, 4.70, 4.90.

Tables 6 and 7 present a comparative assessment of the Nakagami and SS-Nakagami models based on log-likelihood values and several goodness-of-fit criteria. For both the glass fibre and carbon fibre datasets, the proposed SS-Nakagami distribution consistently demonstrates superior performance relative to the classical Nakagami model. This improvement is evidenced by higher log-likelihood values, lower information criteria (AIC and BIC), and smaller goodness-of-fit statistics, including the Kolmogorov–Smirnov (D), Anderson–Darling (AD), and Cramér–von Mises (CVM) measures. In addition, the larger KS p-values indicate stronger agreement between the fitted and empirical distributions. These statistical findings are further reinforced by the visual evidence provided in Figures 5, which illustrates the estimated PDF and CDF of the Nakagami and SS-Nakagami models against the empirical data for both datasets.

The standard errors associated with the parameter estimates are relatively small, suggesting that the estimation procedure is stable and reliable for both models. These findings indicate that the additional shape flexibility introduced through the sine transformation enhances the adaptability of the model, enabling it to more effectively capture both the central tendency and tail behavior of moderately skewed reliability data. Overall, the results highlight the enhanced flexibility and modeling capability of the SS-Nakagami distribution for real-life applications.

7. Conclusion

We propose a sine-transformed extension of the classical Nakagami distribution that preserves its two-parameter structure while enhancing shape flexibility. Structural properties, including hazard modulation and tail asymptotics, are established, showing that the model retains the light-tailed nature of the baseline distribution.

Maximum likelihood estimation is implemented numerically, and simulation results confirm consistency and satisfactory finite-sample performance. Applications to reliability data demonstrate improved goodness of fit relative to the classical Nakagami model, supporting the practical usefulness of the proposed distribution.

Acknowledgements: This study was supported by Faculty of Science and Technology, Thammasat University, Contract No. SciGR 1/2569.

Conflicts of Interest: The authors declare that there are no conflicts of interest regarding the publication of this paper.

References

[1] A. Ahmad, A.A. Rather, O.A. Alqasem, M.E. Bakr, G.T. Mekiso, O.S. Balogun, E. Hussam, A.M. Gemeay, Introducing Novel Arc Cosine-Ψ Class of Distribution with Theory and Data Evaluation Related to Coronavirus, Sci. Rep. 15 (2025), 13069. https://doi.org/10.1038/s41598-025-95084-w.

[2] C. Alexander, G.M. Cordeiro, E.M.M. Ortega, J.M. Sarabia, Generalized Beta-Generated Distributions, Comput. Stat. Data Anal. 56 (2012), 1880–1897. https://doi.org/10.1016/j.csda.2011.11.015.

[3] A. Alzaatreh, C. Lee, F. Famoye, A New Method for Generating Families of Continuous Distributions, METRON 71 (2013), 63–79. https://doi.org/10.1007/s40300-013-0007-y.

[4] A. Alzaatreh, C. Lee, F. Famoye, Family of Generalized Gamma Distributions: Properties and Applications, Hacet. J. Math. Stat. 45 (2016), 869–886. https://doi.org/10.15672/hjms.20156610980.

[5] D.K. Bhaumik, K. Kapur, R.D. Gibbons, Testing Parameters of a Gamma Distribution for Small Samples, Technometrics 51 (2009), 326–334. https://doi.org/10.1198/tech.2009.07038.

[6] M. Bourguignon, R.B. Silva, G.M. Cordeiro, The Weibull-G Family of Probability Distributions, J. Data Sci. 12 (2014), 53–68. https://doi.org/10.6339/jds.201401_12(1).0004.

[7] G.M. Cordeiro, M. de Castro, A New Family of Generalized Distributions, J. Stat. Comput. Simul. 81 (2011), 883–898. https://doi.org/10.1080/00949650903530745.

[8] N. Eugene, C. Lee, F. Famoye, Beta-Normal Distribution and Its Applications, Commun. Stat. Theory Methods 31 (2002), 497–512. https://doi.org/10.1081/STA-120003130.

[9] E. Gómez-Déniz, L. Gómez-Déniz, A New Derivation of the Nakagami-m Distribution as a Composite of the Rayleigh Distribution, Wirel. Netw. 30 (2024), 3051–3060. https://doi.org/10.1007/s11276-024-03713-5.

[10] A.S. Gvozdarev, α-Fluctuating Nakagami-m Fading Model for Wireless Communications, Sensors 25 (2025), 3430. https://doi.org/10.3390/s25113430.

[11] C. Lee, F. Famoye, O. Olumolade, Beta-Weibull Distribution: Some Properties and Applications to Censored Data, J. Mod. Appl. Stat. Methods 6 (2007), 173–186. https://doi.org/10.22237/jmasm/1177992960.

[12] A.W. Marshall, I. Olkin, A New Method for Adding a Parameter to a Family of Distributions with Application to the Exponential and Weibull Families, Biometrika 92 (2005), 505–505. https://doi.org/10.1093/biomet/92.2.505.

[13] A.A. Mir, S.U. Rasool, S.P. Ahmad, A.A. Bhat, T.M. Jawa, N. Sayed-Ahmed, A.H. Tolba, A Robust Framework for Probability Distribution Generation: Analyzing Structural Properties and Applications in Engineering and Medicine, Axioms 14 (2025), 281. https://doi.org/10.3390/axioms14040281.

[14] G.S. Mudholkar, D.K. Srivastava, Exponentiated Weibull Family for Analyzing Bathtub Failure-Rate Data, IEEE Trans. Reliab. 42 (1993), 299–302. https://doi.org/10.1109/24.229504.

[15] M. Nakagami, The m-Distribution—A General Formula of Intensity Distribution of Rapid Fading, in: Statistical Methods in Radio Wave Propagation, Elsevier, pp. 3–36, (1960). https://doi.org/10.1016/B978-0-08-009306-2.50005-4.

[16] M.D. Nichols, W.J. Padgett, A Bootstrap Control Chart for Weibull Percentiles, Qual. Reliab. Eng. Int. 22 (2006), 141–151. https://doi.org/10.1002/qre.691.

[17] P.E. Oguntunde, O.S. Balogun, H.I. Okagbue, S.A. Bishop, The Weibull-Exponential Distribution: Its Properties and Applications, J. Appl. Sci. 15 (2015), 1305–1311. https://doi.org/10.3923/jas.2015.1305.1311.

[18] D.O. Oramulu, N. Alsadat, A. Kumar, M.M. Bahloul, O.J. Obulezi, Sine Generalized Family of Distributions: Properties, Estimation, Simulations and Applications, Alexandria Eng. J. 109 (2024), 532–552. https://doi.org/10.1016/j.aej.2024.09.001.

[19] R.L. Smith, J.C. Naylor, A Comparison of Maximum Likelihood and Bayesian Estimators for the Three-Parameter Weibull Distribution, Appl. Stat. 36 (1987), 358–369. https://doi.org/10.2307/2347795.

[20] L. Tomy, L. Dominic, Review on Distributions Generated Using Trigonometric Functions, Aust. J. Stat. 53 (2024), 102–119. https://doi.org/10.17713/ajs.v53i3.1827.